Quantum Electronics **45** (6) 527–532 (2015)

LASER PLASMA

PACS numbers: 32.30.–r; 52.38.Ph; 52.50.Jm
DOI: 10.1070/QE2015v045n06ABEH015679

Broadening and shift of the spectral lines of hydrogen atoms and silicon ions in laser plasma

N.E. Kask, E.G. Leksina, S.V. Michurin, G.M. Fedorov, D.B. Chopornyak

Abstract. **We report an experimental investigation of the broadening and shift of discrete lines in the plasma spectrum produced in the laser ablation of silicon in a broad pressure range (10^2–10^7 Pa) of the ambient gas (Ar, He, H_2). The broadening and line shifts are measured in relation to the distance from the target and initial gas pressure. The threshold nature of the resulting dependences is found to be related to the formation of virtual percolation clusters proceeding in the hot dense plasma.**

Keywords: *laser ablation, percolation, shift and broadening of spectral lines.*

1. Introduction

According to Zhukhovitskii [1], a dense plasma with a temperature exceeding the boiling temperature of condensed substance may be the site of formation of 'hot' virtual clusters: atomic chains and fractal-like structures. The term 'hot' may also be used in reference to percolation clusters, both critical and subcritical, which emerge in the model of dynamic percolation [2, 3]. The formation of hot clusters changes the optical and electrical characteristics of the plasma. Since percolation is a threshold process, it would appear reasonable that such characteristics as the width, shift, and intensity of spectral lines would exhibit threshold behaviour.

The past 20–30 years have seen numerous investigations of the atomic and ionic spectra of the products of laser ablation, but they have not exhibited threshold-like variations of spectral characteristics. We note that the majority of papers were concerned with the investigation of only the atomic and ionic spectra of target substance, while the changes in the spectra of buffer gases were scarcely studied. However, the reaction of a buffer inert gas to the emergence of hot virtual clusters consisting of the target material atoms would be expected to be more pronounced. The gas atoms, on finding themselves in the immediate vicinity of a cluster, do not enter in its composition and retain their discrete spectrum. Local field fluctuations in the cluster as well as the higher electron density in its immediate vicinity may result in a significant difference of the spectral dependences for the buffer gas from the corresponding dependences for target atoms.

N.E. Kask, E.G. Leksina, S.V. Michurin, G.M. Fedorov, D.B. Chopornyak D.V. Skobel'tsyn Institute of Nuclear Physics, M.V. Lomonosov Moscow State University, Vorob'evy gory, 119991 Moscow, Russia; e-mail: nek@srd.sinp.msu.ru

Received 24 September 2014
Kvantovaya Elektronika **45** (6) 527–532 (2015)
Translated by E.N. Ragozin

The use of hydrogen as a buffer gas shows promise and is of importance for recording the percolation transition. The simplest atom and the most abundant element in the Universe is most often the object of theoretical and experimental research. Its spectra are actively studied in the optical breakdown [4–7]. The broadening of spectral lines is used for determining the electron density in experiments involving laboratory plasmas of different composition and with a purposefully introduced admixture of hydrogen [8]. As a result, vast material has been accumulated for the width and shift of hydrogen spectral lines in relation to different factors, for instance pressure. Since the laser plume is a rather complex object with discontinuities of gas-dynamic parameters in its volume, studying hydrogen spectra in the plasma of ablated substance is of major significance. It is noteworthy that the study of the width and shift of the spectral lines of hydrogen and silicon in dense plasmas is, in particular, of astrophysical interest, because these lines are present in the visible radiation of the Sun and other stars [9].

2. Experimental facility and methods

Silicon was ablated by single ~10-ns pulses of laser radiation with a wavelength of 1.06 μm. The radiation was focused onto the target with a flat-convex lens with a focal length $F = 300$ mm; the focal spot radius was equal to 0.15 ± 0.05 mm. The energy density at the target surface was equal to ~70 J cm^{-2}. We note that the transition from normal vaporisation to a phase explosion [10, 11] is attended with a significant increase in plume luminosity [12] and takes place for a threshold flux density above 19 ± 4 J cm^{-2}.

The target under investigation was placed into a hermetically sealed chamber (the inner diameter and length were equal to 25 and 150 mm). The buffer gas pressure p_b in the chamber could be varied from 0.001 to 100 atm; for a buffer gas, we used hydrogen, helium, and argon.

We investigated the spectrum and intensity of laser plasma radiation propagating in two directions: longitudinal, in opposition to the laser beam, and transverse, perpendicular to the plume axis. In the latter case, we recorded the emission of a plasma layer located at a selected distance from the target surface. The spatial resolution was equal to ~100 μm. Time-integrated spectra were obtained using a diffraction grating spectrometer (600 grooves mm^{-1}). The slit width was equal to 30 μm and the spectral resolving power $\lambda/\delta\lambda \approx 24000$. The spectra were studied in a wavelength range $350 < \lambda < 900$ nm. The width of recorded spectral range was determined by the focal distance F of a collecting lens. With an $F = 800$ mm lens, a spectral interval of ~50 nm was imaged onto a CCD linear array. This interval is sufficiently broad (Fig. 1) to encompass the 634.7- and 637.1-nm spectral lines of silicon and the

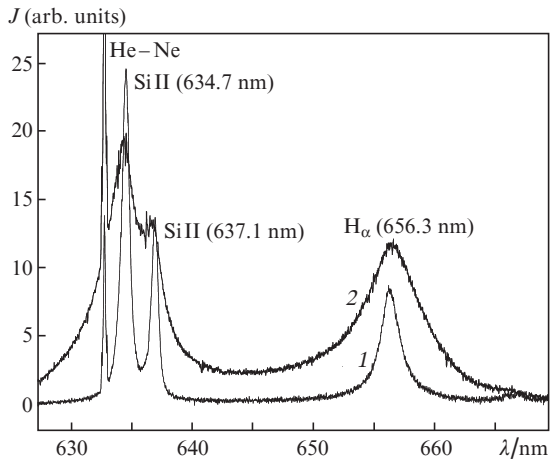

Figure 1. Silicon and hydrogen spectra for buffer gas pressures of (*1*) 1 and (*2*) 5 atm, and He–Ne laser line.

656.3-nm line of hydrogen (the H_α Balmer line). This circumstance allowed us to study and compare the line shifts relative to each other in one experimental realisation.

The longitudinal radiation, which propagated in opposition to the laser beam and was integrated over the entire volume of the plasma cloud, was directed to the input of an SFL-451 spectrofluorimeter with the spectral operating range $400 < \lambda < 900$ nm and a resolution of 6.4 nm. The resultant spectra permitted us to compare the intensities of different spectral lines and the continuous plasma emission.

Konjevic [13] formulated the reliability criteria for plasma diagnostic techniques based on measurements of the broadening and shift of spectral lines. Required, in particular, are the uniformity of the plasma region under study, its stationarity during the measurement period, and the existence of local thermodynamic equilibrium. The plasma produced in the laser ablation by the pulses of nanosecond duration is characterised both by nonuniformity and nonstationarity, and local thermodynamic equilibrium is broken near the discontinuity surfaces of gas-dynamic parameters. A high substance density in the plume is attended with different instabilities, intermittency, and turbulence.

Different plasma spectroscopic techniques were developed to minimise these difficulties. Wide use is made of spectroscopy with a high temporal resolution. In the case of a phase explosion and an explosion wave, which occur in the ablation by nanosecond-long laser pulses, the most significant changes take place near the discontinuity surfaces of gas-dynamic parameters. The high motion velocity of these surfaces permits using spatial resolution instead of the temporal one: a time interval of 100 ns, which is typical for experiments with temporal resolution, corresponds to a spatial interval of 1 mm when the explosion wave velocity is equal to $\sim 10^4$ m s^{-1}.

3. Density variation in a laser plume

3.1. Explosion wave

Nonstationary wave motion for a point explosion was first considered by the authors of Refs [14, 15]. In the case of a strong point explosion, the wave motion is self-similar and it is possible to obtain an analytical solution in the case of adiabaticity and one-dimensionality of motion [16]. The key parameters for the description of velocity, density, and pressure profiles behind the wave front are, apart from the time, the energy delivered to the target surface, the adiabatic exponent of the ambient gas, and its density. The two last-named parameters, as well as the sound velocity and the initial gas density related by the adiabatic equation, characterise one of stagnation points of the problem. This point is located ahead of the explosive wave and its parameters are denoted by subscript 0 [17]. In the present work, subscript 3 is employed for the corresponding parameters of another stagnation point, which is located immediately at the target surface. Subscripts 1 and 2 correspond to the shock wave front and the contact surface between the plasma and the buffer gas.

The strength of a shock wave and its many other parameters are defined in terms of the pressure ratio p_1/p_0. A shock wave is termed strong when its velocity is ten or more times greater than the sound velocity in the surrounding medium (the Mach number $M \geqslant 10$, $p_1/p_0 \geqslant 100$). In the passage of a shock wave, the density of the medium is relatively little changed [14–17]. The buffer gas at the front of a strong shock wave obeys the following relation (neglecting ionisation and dissociation):

$$\frac{\rho_1}{\rho_0} = \frac{\gamma_0 + 1}{\gamma_0 - 1}. \tag{1}$$

For a monoatomic gas, its density increases four-fold at this discontinuity.

3.2. Rarefaction wave

The vapour behind the contact surface may be treated as a working gas, whose expansion forms a shock wave in the surrounding gas. A discontinuity of gas-dynamic variables is formed at the contact surface: the density and temperature undergo a step-like change, while the pressure and velocity are continuous. According to Refs [17, 18], in this case there applies the following inequality:

$$\frac{\rho_0}{\rho_3} \ll \frac{(\gamma_3 - 1)^3}{2\gamma_3(\gamma_0 + 1)}, \tag{2}$$

whose fulfilment necessitates that the vapour density should be at least two orders of magnitude higher than the ambient gas density. It is also known that a rarefaction wave propagates toward the target through the domain occupied by the vapour [17]. In the laboratory frame of reference, for every local point its velocity is defined by the difference of the local flow velocity u, which is directed away from the target, and the local sound velocity [16, 17]:

$$u - a = u - a_3 + \frac{\gamma_3 - 1}{2}u. \tag{3}$$

For an ideal gas with a constant heat capacity, the following relations hold for a centred rarefaction wave [17]:

$$\frac{a}{a_3} = 1 - \frac{\gamma_3 - 1}{2}\frac{u}{a_3}, \tag{4}$$

$$\frac{p}{p_3} = \left(1 - \frac{\gamma_3 - 1}{2}\frac{u}{a_3}\right)^{2\gamma_3/(\gamma_3 - 1)}, \tag{5}$$

$$\frac{T}{T_3} = \left(1 - \frac{\gamma_3 - 1}{2}\frac{u}{a_3}\right)^2, \quad (6)$$

$$\frac{\rho}{\rho_3} = \left(1 - \frac{\gamma_3 - 1}{2}\frac{u}{a_3}\right)^{2/(\gamma_3 - 1)}, \quad (7)$$

where the variables without a subscript refer to local parameters of the rarefaction wave. When the rarefaction wave propagates through the monoatomic vapour of the target material, its density is much (by more than a factor of 10, [16]) higher than the density of the surrounding gas. Account should be taken of the fact the formation of dimers, trimers, etc. in the dense gas leads, according to expressions (4)–(7), to an increase in all parameters of the rarefaction wave. The following approximation holds good for polyatomic nonlinear molecules whose all vibrational and rotational degrees of freedom are excited [19]:

$$\gamma \approx (3N - 2)/(3N - 3). \quad (8)$$

As the number of atoms N in molecules increases, the adiabatic index approaches unity and the magnitudes of subscript-free parameters in formulas (4)–(7), which are calculated with participation of formula (8), become higher (Fig. 2). In the calculation of the dependences plotted in Fig. 2, the data on the characteristics of the laser plume were borrowed from Ref. [16]. At the effective number of atoms $N_{\text{eff}} \sim 6$, the density in the medium, as compared to single-atom vapour, increases by 16 times.

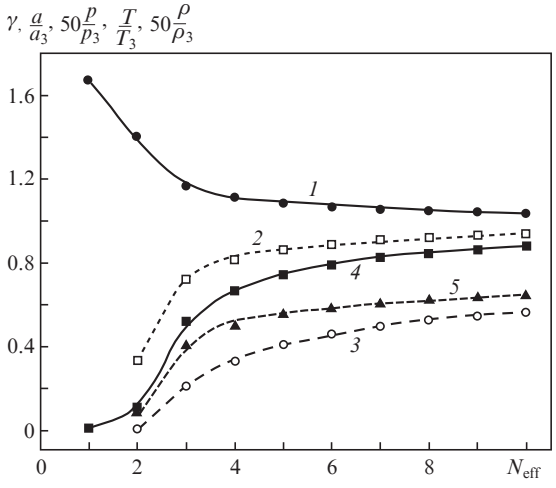

Figure 2. Dependences of the effective adiabatic index γ (*1*) as well as of rarefaction wave parameters a/a_3 (*2*), $50p/p_3$ (*3*), T/T_3 (*4*), and $50\rho/\rho_3$ (*5*) on the effective number of atoms in the clusters of ablated material [see formulas (4)–(8)].

According to Ref. [20], for percolation to occur in a Coulomb system, the density must be close to the critical one, which is equal to 750 ± 100 kg m^{-3} for silicon [21]. At normal conditions, the respective densities of surrounding gases H_2, He, and Ar are equal to 0.09, 0.179, and 1.784 kg m^{-3}. In view of inequality (2) and relation (7), the critical density of ablated material (silicon) may be reached for the normal pressure of the surrounding Ar gas. For He and H_2, it will take external pressure 10–20 times higher than the normal one, which is consistent with the data of our experiments [22–26]. To do this requires that polyatomic molecules (clusters) are efficiently produced in the region where the rarefaction wave takes place.

4. Formation of fractal structures in a laser plume

Earlier we observed the formation of fractal, in particular percolative, structures in the ablation of silicon and different metallic targets by quasi-continuous laser radiation with a duration of ten milliseconds [22–24]. Linear and fractal microclusters accumulated in cold peripheral plume layers with irradiation of so long a pulse [22–24]. For sufficiently low (below two atmospheres) pressures of the surrounding gas, it was possible to observe the deposition of microclusters on the chamber walls and a specially introduced glass substrate for ten–fifteen minutes upon cessation of the laser pulse. When the initial gas (argon) pressure in the sample-containing chamber was higher than two atmospheres, sufficiently many fractal structures managed to accumulate in the outer layer of the laser plume during laser irradiation, so that their density exceeded the percolation threshold. As a result, the microclusters merged into a linked fractal shell, which did not disintegrate into parts upon termination of the laser pulse and found itself on the substrate [22–24]. When use was made of helium as the ambient gas, the threshold pressure required to trigger the formation of the linked fractal shell increased to ten atmospheres [22].

A similar behaviour of spectral line intensities in relation to the pressure of the ambient atmosphere is also observed in the ablation of different targets by pulsed laser radiation of nanosecond duration. Figure 3 shows experimental data obtained in the ablation of silicon and copper targets in the atmosphere of argon. This plot serves to illustrate the similarity of the dependences obtained for different targets, the difference in positions on the pressure scale between the intensity peaks of the discrete spectra of argon and target substance, as well as the coincidence on the pressure axis between the intensity peaks of the buffer gas and continuum spectra. It should be added that the like behaviour was also observed for other metals under our investigation: Al, Ag, Mg, Ti, etc. In the ablation in the atmosphere of helium, the intensity peaks take place at pressures approximately five times higher than in the ablation in argon atmosphere. The same pressure ratio with replacement of Ar by He is observed under 10-ms long quasi-continuous irradiation [22, 24]. Of significance is the fact that the positions of peaks on the pressure axis remain invariable as the pulse duration is changed by a factor of $\sim 10^6$ (provided the gas is the same).

Also noteworthy are the differences which manifest themselves in experiments for the specifies ablation regimes. Unlike the irradiation by a millisecond pulse, when a linked fractal shell is formed on reaching the threshold pressure, in the case of nanosecond irradiation we failed to discover the corresponding fractal structures in experiments. It is likely that there exists a strong coupling between the dense plasma and the target surface in the phase explosion. Under millisecond irradiation [25], for some metals (Ni, Re, Pb) a similar effect gives rise to porous cones on the target surface, where characteristic craters are observed in the majority of experiments. Interestingly, in the ablation by higher-power femtosecond pulses it was determined that ramified nanoclusters are formed in a time shorter than 10 ns [27].

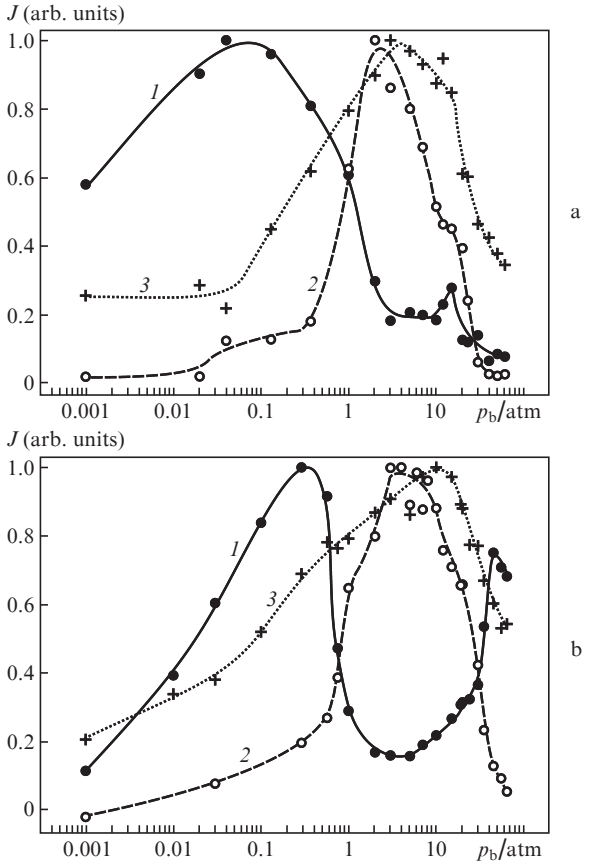

Figure 3. Intensities J of the spectral lines of (*1*) target substance and (*2*) buffer gas, as well as of (*3*) continuum as functions of the surrounding atmospheric pressure p_b for (a) a silicon target and an argon buffer gas and (b) for a copper target and an argon buffer gas. The intensities are normalised to the corresponding peak values.

The outlined data are indicative of the possible similarity of percolation structure formation mechanisms for the specified laser ablation regimes. It is noteworthy that this similarity of processes that take place on different scales (spatial and temporal) is a characteristic property of fractals, in particular in the percolation [28].

5. Shift and broadening of spectral lines

5.1. Broadening of hydrogen and silicon spectral lines in relation to the pressure

In Ref. [26] it was determined that the pressure dependences of the broadening of the spectral lines of a buffer gas are significantly different from the corresponding dependences for the atoms and ions of the target material. In comparison with the radiation of the target atoms, the radiation of buffer gas atoms emanates from higher-density plasma layers and their spectral line profiles are complex in shape. The profile of the broadened spectral lines of target substance is quite accurately described by a single Lorentzian profile. In the case of a buffer gas, a single-profile approximation describes experimental profiles adequately only for relatively low pressures: below 2 atm for argon and below 10 atm for helium. At higher initial pressures, a rather good (to better than 10%) approximation of the profile of a discrete line is provided by its expansion into two Lorentzian profiles. Figure 4 shows the dependences obtained by approximating the investigated hydrogen line profile by one and two Lorentzian profiles. Both approximations clearly demonstrate the threshold-like behaviour of the dependences on the buffer gas pressure: a characteristic knee is observed for a threshold pressure $p_{tr} \approx 2.5$ atm.

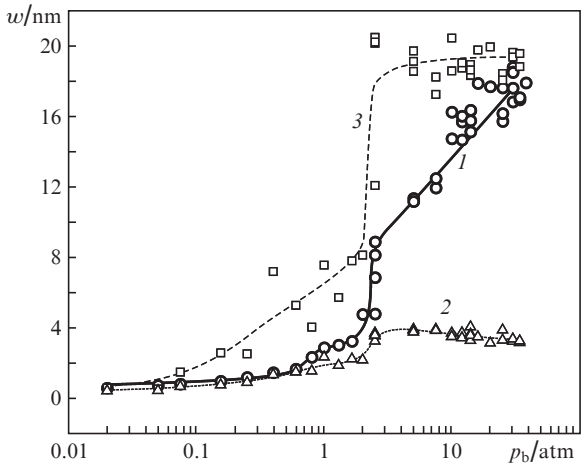

Figure 4. Dependence of the half-width w of the hydrogen spectral line on the initial pressure of the surrounding atmosphere with profile approximation by (*1*) one and (*2*, *3*) two Lorentzian profiles.

Figure 5 shows the pressure dependences of the broadening of silicon spectral lines in the atmosphere of hydrogen and argon. In the analysis of the line shapes, use was made of the single-profile approximation. It is noteworthy that the changes of the half-width of silicon spectral line are significantly smaller than those observed for hydrogen. Calculations of the Stark line broadening based on the well-known expressions and tables [29] lead to the following conclusion. Up to a certain threshold, to which there corresponds a pressure of ~2.5 atm, the radiating hydrogen and argon atoms as well as silicon ions are in the plasma domain where the free-electron density is equal to $\sim 10^{17}$ cm^{-3}. Above the threshold, the main contribution to hydrogen and argon radiation is made by the atoms which reside in the plasma with a higher electron density ($\sim 10^{18}$ cm^{-3}). It would be reasonable to assume that the atoms and ions of the target substance radiate from the layers

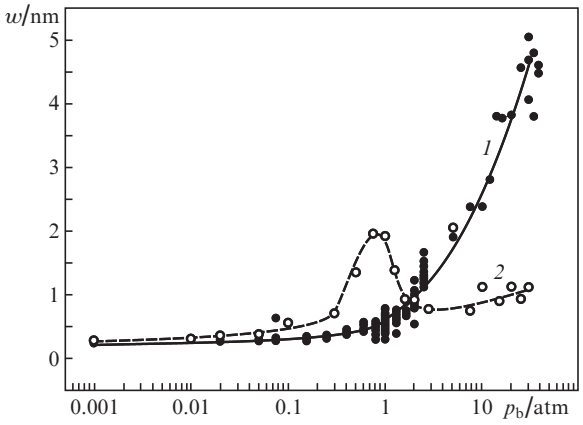

Figure 5. Dependences of the half-width w of the $\lambda = 634.7$ nm silicon spectral line on the initial pressure of (*1*) hydrogen and (*2*) argon. The line profiles were approximated by a single Lorentzian profile.

adjacent to the contact surface for sufficiently low pressures, when the plasma density is below the percolation threshold. As a whole, the volume occupied by the plasma is optically thick and is characterised by continuum radiation. When the plasma density of the layer adjacent to the contact surface exceeds the percolation threshold, the densities of free atoms and ions of the target substance become substantially lower. The buffer gas atoms are almost invariable in number, because they are not parts of clusters. The higher electron density in the layer behind the contact surface gives rise to the broadening of buffer gas spectral lines.

5.2. Shifts of silicon and hydrogen spectral lines in relation to the pressure

A high electron density [6, 7], the existence of its gradients in laser plasmas, and the specificity of transfer processes at the threshold of percolation [30] underlie the interest in studying spectral line shifts in laser ablation. Figures 6 and 7 show respectively the experimental pressure dependences of the shifts of the 634.7-nm silicon ion line and the H_α hydrogen line. A single-profile approximation was employed for the silicon spectral line (Fig. 6), and single- and two-profile approximations for the H_α line (Fig. 7). The dependences obtained in the silicon ablation in the atmospheres of hydrogen and argon are compared in Figs 5 and 6. As these plots suggest, not only does the buffer gas determine the position of the threshold on the density axis, but it also affects the width and shift of the spectral lines of the target material. This difference is primarily observed at above-threshold pressures. It is noteworthy that hydrogen, unlike a rare gas, may also participate in the formation of percolation clusters as a chemically active element.

The character of dependences plotted in Figs 6 and 7 changes markedly on exceeding the threshold pressure. Where percolation takes place, the majority of silicon ions are parts of clusters, while the solitary ions, which radiate a discrete spectrum, are spatially remote from this domain. The dependence nevertheless becomes more wavy in comparison, for instance, with the dependence for the H_α line at the same pressures (Fig. 7). The possible reason may lie with the emergence of silicon ions near a contact surface, which also is a fractal object. The dimensionality of this fractal coincides with the dimensionality of the percolation clusters located in the plasma volume [31]. The dynamic nature of hot percolation cluster formation (their decay and restructuring) has the effect that fluctuations are inherent in cluster growth and decay in the volume and surface layer of the plasma [2].

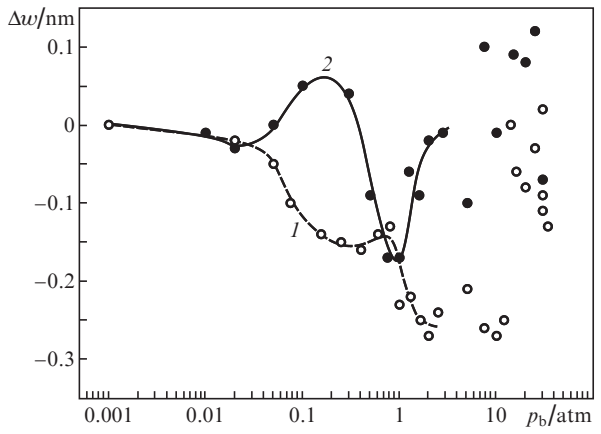

Figure 6. Dependences of the shift Δw of the $\lambda = 634.7$ nm silicon spectral line on the initial pressure of (*1*) hydrogen and (*2*) argon. The line profiles were approximated by a single Lorentzian profile.

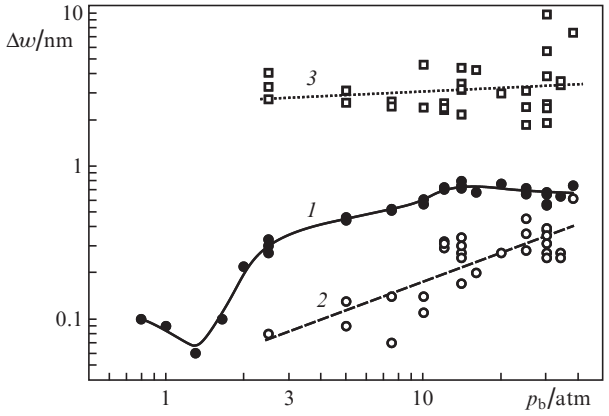

Figure 7. Dependences of the shift Δw of the $\lambda = 656.3$ nm hydrogen spectral line on the initial pressure of the surrounding atmosphere with line profile approximation by (*1*) one and (*2*, *3*) two Lorentzian profiles.

5.3. Broadening and shift of spectral lines in relation to the distance from the target

The density of ablated substance cloud decreases with distance from the target due to expansion and recombination of plasma components. In the investigation of the broadening and shift of spectral lines in relation to the distance from the target, for a sufficiently high pressure it is possible to pass through the threshold domain and, on the one hand, obtain information about the percolation structures and electron density as the contact surface recedes from target and, on the other, estimate the electron density gradient near the contact surface.

Figure 8 shows the spatial dependences of the broadening and shift of the hydrogen line under study, which were obtained for initial pressures exceeding the threshold one. The two profiles which approximate the line profile differ widely in half-width and shift. For the narrow profile, the shift is negligible and the half-width increases monotonically. Characteristic of the broad profile are an alternating-sign shift and unexpectedly strong changes of the half-width with approach to the target surface. In this case, the line shift, measured simultaneously with the half-width, changes only slightly within the uncertainty of the two-profile approximation. By contrast, the pulsations are stronger pronounced for the line-shift dependences with variation of the initial pressure (see Fig. 7). The data shown in Fig. 8 suggest that the electron density is highest at some distance from the surface and decreases on either side of this point with about the same gradient.

6. Conclusions

The broadening and shift of the spectral lines of a buffer gas and target substance were first compared in the plasma pro-

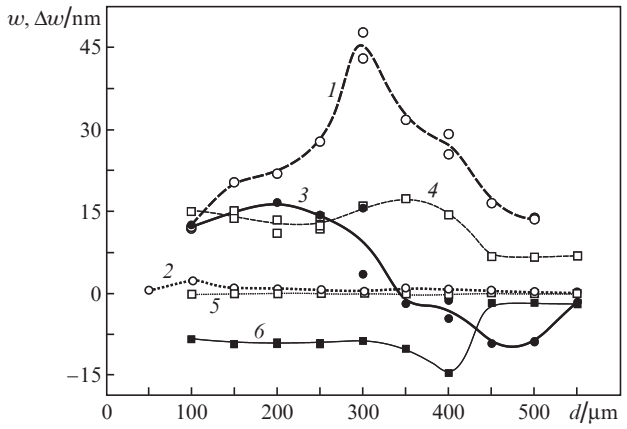

Figure 8. Dependences of the half-width w of (*1*, *4*) the broad profile as well as of the shifts Δw of (*2*, *5*) the narrow and (*3*, *6*) broad profiles, which were obtained in the decomposition of the spectral line of ambient gas, on the distance d from the target surface: (*1*–*3*) Si target, the initial hydrogen pressure is equal to 45 atm, $\lambda = 656.3$ nm, and (4–6) a Cu target, the initial helium pressure is equal to 40 atm, $\lambda = 587.6$ nm.

duced by laser ablation. Our experimental investigations were mostly carried out for a silicon target placed in a hydrogen atmosphere. It was determined that the dependences of the half-width and shift of the spectral line of a buffer gas on the pressure and distance from the target exhibit threshold-like behaviour. The threshold is due to the formation of percolation clusters of atoms and ions of the target material in a dense plasma, the discrete lines of the target material practically vanishing from the optical spectra of the plasma. The threshold-like behaviour, which is characteristic for the spectral line of the buffer gas, is attended with the broadening, shift, and asymmetry of its profile. Above the threshold, the density fluctuations of electron plasma component were found to result in the instability of the broadening of the spectral line of the surrounding gas in the domain where percolation took place.

References

1. Zhukhovitskii D.I. *Zh. Eksp. Teor. Fiz.*, **113**, 181 (1998) [*JETP*, **86**, 101 (1998)].
2. De Freitas J.S., Lucena L.S., Roux S. *Physica A*, **266**, 81 (1999).
3. Alencar A.M., Andrade J.S., Lucena L.S. *Phys. Rev. E*, **56**, R7359 (1997).
4. Böddeker St., Günter S., Könies A., Hitzschke L., Kunze H.-J. *Phys. Rev. E*, **47**, 2785 (1993).
5. Parriger C.G., Lews J.W.L., et al. *J. Quant. Spectrosc. Radiat. Transfer*, **53**, 249 (1995).
6. Parriger C.G., Plemmons D.H., Oks E. *Appl. Opt.*, **42**, 5992 (2003).
7. Parriger C.G., Oks E. *Int. Rev. Atomic Molecular Phys.*, **1**, 13 (2010).
8. Janus H.W. *J. Phys. D: Appl. Phys.*, **40**, 3608 (2007).
9. Gonzalez V.R., Aparicio J.A., et al. *J. Phys. B: At. Mol. Opt. Phys.*, **35**, 3557 (2002).
10. Geohegan D.B. *Appl. Phys. Lett. A*, **69**, 1463 (1993).
11. Yoo J.H., Jeong S.H., Mao X.L., et al. *Appl. Phys. Lett.*, **76**, 783 (2000).
12. Bulgakova N.M., Bulgakov A.V. *Appl. Phys. A*, **73**, 199 (2001).
13. Konjevic N. *Plasma Sources Sci. Technol.*, **10**, 356 (2001).
14. Sedov L.I. *Similarity and Dimensional Methods in Mechanics* (New York: Academic Press, 1959; Moscow: Nauka, 1967).
15. Taylor G.I. *Proc. R. Soc. A*, **201**, 159 (1950).
16. Zhang Z., Gogos G. *Phys. Rev. B*, **69**, 235403 (2004).
17. Zel'dovich Ya.B., Raizer Yu.P. *Physics of Shock Waves and High-Temperature Hydrodynamic Phenomena* (New York: Academic Press, 1966, 1967; Moscow: Nauka, 1966) Vols 1, 2.
18. Velikovich A.L., Liberman M.A. *Fizika udarnykh voln v gazakh i plazme* (Physics of Shock Waves in Gases and Plasma) (Moscow: Nauka, 1987).
19. Brykin M.V., Vorob'ev V.S., Shelyukhaev B.P. *Teplofiz. Vys. Temp.*, **25**, 468 (1987).
20. Likal'ter A.A. *Usp. Fiz. Nauk*, **170**, 831 (2000) [*Phys. Usp.*, **43**, 777 (2000)].
21. Honda N., Nagasaka Y. *Int. J. Thermophys.*, **20**, 837 (1999).
22. Kask N.E., Leksina E.G., Michurin S.V., Fedorov G.M., Chopornyak D.B. *Kvantovaya Elektron.*, **32**, 437 (2002) [*Quantum Electron.*, **32**, 437 (2002)].
23. Kask N.E., Leksina E.G., Michurin S.V., Fedorov G.M. *Kvantovaya Elektron.*, **37**, 366 (2007) [*Quantum Electron.*, **37**, 366 (2007)].
24. Kask N.E., Leksina E.G., Michurin S.V., Fedorov G.M. *Laser Phys.*, **18**, 762 (2008).
25. Kask N.E., Leksina E.G., Michurin S.V., Fedorov G.M., Chopornyak D.B. *Kvantovaya Elektron.*, **35**, 347 (2005) [*Quantum Electron.*, **35**, 347 (2005)].
26. Kask N.E., Michurin S.V. *Kvantovaya Elektron.*, **42**, 1002 (2012) [*Quantum Electron.*, **42**, 1002 (2012)].
27. Gamaly E.G., Madsen N.R., Golberg D., Rode A.V. *Phys. Rev. B*, **80**, 184113 (2009).
28. Feder J. *Fractals* (New York: Plenum Press, 1988; Moscow: Mir, 1991).
29. Griem H.R. *Spectral Line Broadening by Plasmas* (New York: Academic Press, 1974; Moscow: Mir, 1978).
30. Zelenyi L.M., Milovanov A.V. *Usp. Fiz. Nauk*, **174**, 809 (2004) [*Phys. Usp.*, **47**, 749 (2004)].
31. Rosso M., Gouyet J.F., Sapoval B. *Phys. Rev. B*, **32**, 6035 (1985).